This article was downloaded by:
On: *14 January 2011*
Access details: *Access Details: Free Access*
Publisher *Taylor & Francis*
Informa Ltd Registered in England and Wales Registered Number: 1072954 Registered office: Mortimer House, 37-41 Mortimer Street, London W1T 3JH, UK

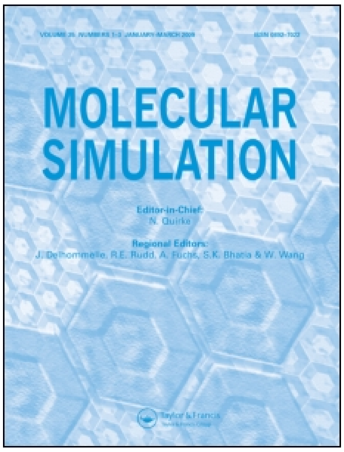

Molecular Simulation

Publication details, including instructions for authors and subscription information:
http://www.informaworld.com/smpp/title~content=t713644482

Diffusivity of CH_4 In Model Silica Nanopores: Molecular Dynamics and Quasichemical Mean Field Theory

George K. Papadopoulos[a]
[a] School of Chemical Engineering, National Technical University of Athens, Athens, Greece

To cite this Article Papadopoulos, George K.(2005) 'Diffusivity of CH_4 In Model Silica Nanopores: Molecular Dynamics and Quasichemical Mean Field Theory', Molecular Simulation, 31: 1, 57 — 66
To link to this Article: DOI: 10.1080/08927020512331325783
URL: http://dx.doi.org/10.1080/08927020512331325783

PLEASE SCROLL DOWN FOR ARTICLE

Full terms and conditions of use: http://www.informaworld.com/terms-and-conditions-of-access.pdf

This article may be used for research, teaching and private study purposes. Any substantial or systematic reproduction, re-distribution, re-selling, loan or sub-licensing, systematic supply or distribution in any form to anyone is expressly forbidden.

The publisher does not give any warranty express or implied or make any representation that the contents will be complete or accurate or up to date. The accuracy of any instructions, formulae and drug doses should be independently verified with primary sources. The publisher shall not be liable for any loss, actions, claims, proceedings, demand or costs or damages whatsoever or howsoever caused arising directly or indirectly in connection with or arising out of the use of this material.

Molecular Simulation, Vol. 31 (1), 15 January 2005, pp. 57–66

Taylor & Francis
Taylor & Francis Group

Diffusivity of CH_4 In Model Silica Nanopores: Molecular Dynamics and Quasichemical Mean Field Theory

GEORGE K. PAPADOPOULOS*

School of Chemical Engineering, National Technical University of Athens, GR 15780 Zografou Campus, Athens, Greece

(Received September 2004; In final form September 2004)

Equilibrium molecular dynamics and dual control volume grand canonical molecular dynamics experiments were carried out aiming at the investigation of the dependence of transport diffusivity upon the adsorbent pore size and sorbate concentration of CH_4 in cylindrical silica nanopores at 298 K, calibrated with respect to experimental data of zeolite VPI 5; the results of simulation were elaborated on the basis of the quasichemical mean field approximation via a theoretical model for surface diffusion. Our mapping procedure between simulation and quasichemical theory reveals that sorbate–sorbate energetics emerge as the physical reason for the variation of corrected (Darken) and hence transport diffusivity with respect to pore size and sorbed phase fractional occupancy.

Keywords: Molecular dynamics; Dual control volume grand canonical molecular dynamics; Nanopores; Transport diffusivity; Corrected diffusivity; Quasichemical mean field approximation

INTRODUCTION

In the literature one finds considerable amount of work concerning experimental and theoretical studies of confined fluids (sorbates) in nanoporous materials. Recently, computer simulation studies of such systems in a molecular level, given a model for the interaction energetic for all the molecular species present, have contributed significantly to a better understanding of many aspects of the equilibrium and kinetics of the sorbed phase.

Previous simulation studies have predicted successfully the sorption and diffusion of several gases in microporous amorphous substrates by modeling a part of their pore structure (e.g. single pores of various geometries) [1,2], and in zeolites by atomistic representation of their crystal unit [3–7]. More sophisticated functions for the potential energy including many body interactions have also been used [7]. The modeling of the interactions with the solid surface, has been done by exploiting either pairwise additive or analytical expressions for the potential energy exerted by the atoms of the surface on an adsorbate molecule [8,9]; an alternative strategy adopted in this work is the suitable calibration of the model surface with respect to experimental data such as the energy of adsorption of a given fluid under similar conditions with the simulation experiment [10,21].

The main simulation methods dealing with transport studies under nonequilibrium conditions, inside the linear response regime of the system after an external perturbation, can be classified in two categories. The first deals with flow driven by an external force field, acting in one direction on the adsorbate molecules resembling this way to the gravitational one [4,5,14,33,38,39]. The other category followed in this paper employs concentration gradient as a driving force, modeling in a more realistic form a real permeation experiment [11,12,15–20,32,33]. Other nonequilibrium MD schemes, based on creation of density gradients not across a single pore model but across a whole medium have also been considered. MacElroy's MD method [17] examined the diffusion of hard spheres through a model overlapping spheres micropore membrane, and showed that in very fine pores slip flow rather viscous shear is the predominant mechanism governing the permeation. Pohl *et al.* [18], used such a method over a model silicalite

---

*Corresponding author. Tel.: +30-21-07723112. Fax: +30-21-07723112. E-mail: gkpap@chemeng.ntua.gr

ISSN 0892-7022 print/ISSN 1029-0435 online © 2005 Taylor & Francis Ltd
DOI: 10.1080/08927020512331325783

membrane system in order to study the molecular sieving nature of zeolite and compared their results with permeation experiments.

The method employed in the present paper is based in the dual control volume grand canonical molecular dynamics (DCV GCMD) originally developed by Cracknell *et al.* [11], applied in studies of transport of methane through single slit-shaped pores. Later applications of the method include studies of mixtures in graphite slits [19] and carbon nanopores [20]. In addition to the calculation of the transport diffusion coefficient via DCV GCMD, we have also computed the collective diffusion coefficient D_0 via EMD by tracking the temporal evolution of the center of mass of the fluid. Suh and Nicholson [23], found a strong influence of the wall potential on D_0 of a Lennard-Jones fluid in model slit pores.

Atomistic computer simulation of transport belongs to the category of "microscopic" techniques. Consequently, its results can be compared directly to those from pulsed field gradient-nuclear magnetic resonance (PFG-NMR) and quasielastic neutron scattering (QENS) measurements. Comparison between molecular dynamics simulation and PFG-NMR or QENS experiments are usually conducted at the level of the self-diffusivity, D_s [4,5]. In practical separations and catalytic applications, however, it is the transport diffusivity, D_t, which is of greater importance. Our recent molecular dynamics study along with coherent QENS measurements, regarding the occupancy dependence of D_t, and the corrected diffusivity, D_0, of CO_2 and N_2 in silicalite, showed that their diffusivities are explainable on the basis of different pair interaction energy of the two sorbates [13].

Scope of this work is to show that sorbate pair interaction energy and diffusivity in nanostructures are also affected by the potential field of the individual pore space for the same sorbate. For this purpose, (i) equilibrium and DCV GC molecular dynamics experiments were carried out for the prediction of self-, corrected and transport diffusivity of methane in three sizes of cylindrical silica model nanopores, (ii) the quasichemical mean field approximation [34,35] was adapted in the sorbed phase in order to introduce sorbate–sorbate interactions to the sorption thermodynamics of the system, and (iii) the model of Reed and Ehrlich [36] for surface diffusion on a 3D lattice, in combination with the results of (ii), was employed towards a comparison with the simulation results of (i).

THEORY

Macroscopic Transport

A general expression for the isothermal steady-state single component sorbate flow in the absence of external force fields can be written in Fickian form as follows

$$\mathbf{J} = -D_t(\rho)\nabla\rho \tag{1}$$

Vector **J**, is the mass flux, i.e. the number of molecules flowing per unit area of the nanoporous material due to a concentration (number density ρ) gradient, and D_t is the transport (Fickian) diffusion coefficient, which in general can be a function of concentration.

Under the irreversible thermodynamics formalism, wherein the gradient of chemical potential over thermal energy acts as the driving force for diffusion of the sorbate species, Eq. (1) can be equivalently written as follows

$$\mathbf{J} = -\beta\rho D_0(\rho)\nabla\mu \tag{2}$$

where $\beta = 1/k_B T$, $k_B = R/N_L$ is the Boltzmann constant, and N_L is Avogadro's number. The chemical potential gradient can be expressed as

$$\nabla\mu = \frac{1}{\beta f}\nabla f \tag{3}$$

with f being the fugacity of the sorbed fluid at the considered position.

After manipulation and combination with Eq. (3), Eq. (2) reads

$$\mathbf{J} = -D_t(\rho)\beta\rho\frac{\partial\ln\rho}{\partial\ln f}\nabla\mu \tag{4}$$

Comparison of Eqs. (2) and (4) leads to the following relation

$$D_t(\rho) = D_0(\rho)\frac{\partial\ln f}{\partial\ln\rho} \tag{5}$$

Equation (5), with $D_0(\rho)$ replaced by D_s is known as the Darken approximation.

Statistical Mechanics

The self diffusion coefficient is essentially the one that would be measured by a tracer, or by experiments such as PFG-NMR or QENS, and is related to the correlation of the velocity of a molecule $\mathbf{v}_i(t)$ at time t, with the velocity of the same molecule at some earlier time $\mathbf{v}_i(0)$ according to Green-Kubo expression:

$$D_s = \frac{1}{d_o}\int_0^\infty dt\langle\mathbf{v}_i(t)\cdot\mathbf{v}_i(0)\rangle \tag{6}$$

where d_o is a dimensionality factor (3 for a bulk system, 2 for slit pores and 1 for cylinders). An alternative to the Eq. (6) is the Einstein formula, where the mean squared displacement of all the molecules in the system is averaged, i.g.

$$D_\mathrm{s} = \frac{1}{2d_o} \lim_{t\to\infty} \frac{\mathrm{d}}{\mathrm{d}t} \langle [\mathbf{r}_i(0) - \mathbf{r}_i(t)]^2 \rangle \tag{7}$$

The collective diffusivity is related to fluctuations in velocity of the center of mass of the fluid in analogy to the set of the above equations as follows:

$$D_0 = \frac{N}{d_o} \int_0^\infty \mathrm{d}t \langle \mathbf{u}(t) \cdot \mathbf{u}(0) \rangle \tag{8}$$

$$D_0 = \frac{N}{2d_o} \lim_{t\to\infty} \frac{\mathrm{d}}{\mathrm{d}t} \langle [\mathbf{R}(0) - \mathbf{R}(t)]^2 \rangle \tag{9}$$

where $\mathbf{u}(t)$ is the center-of-mass velocity of the swarm of N molecules, which can be identified with the macroscopic streaming velocity of the system, i.e.

$$\mathbf{u}(t) = \frac{1}{N} \sum_{i=1}^{N} \mathbf{v}_i(t)$$

Clearly, $\mathbf{u}(t) = \dot{\mathbf{R}}(t)$ with $\mathbf{R}$ being the center-of-mass of the swarm of N molecules.

As sorbate loading tends to infinite dilution, obviously cross-correlation functions between velocities of different molecules approach zero and the autocorrelation terms (self-diffusivity) predominate. Also, the sorption isotherm approaches the linear (Henry's law) regime. In this limit,

$$\lim_{\rho\to 0} D_0(\rho) = \lim_{\rho\to 0} D_\mathrm{t}(\rho) = \lim_{\rho\to 0} D_\mathrm{s}(\rho)$$

In the present work, along with a direct estimation of an overall transport diffusion coefficient, through DCV GCMD, we have also utilized the Eqs. (8) and (9) in order to calculate directly D_0 and hence a conjugate D_t from Eq. (5).

SIMULATION METHODOLOGY

Representation of Potentials

Methane was modeled as a 12–6 Lennard-Jones molecule with the potential parameters $\varepsilon/k_\mathrm{B} = 148\mathrm{K}$ and $\sigma = 0.3812\,\mathrm{nm}$ [21] and the intermolecular interactions were calculated by the following effective pair potential

$$U^{\mathrm{LJ}}(r_{ij}) = 4\varepsilon_{ij} \left[\left(\frac{\sigma_{ij}}{r_{ij}} \right)^{12} - \left(\frac{\sigma_{ij}}{r_{ij}} \right)^{6} \right]$$

For the modeling of cylindrical pores we started from an atomistic scale employing a model of "pseudo atoms" [10,21]. It uses an array of interaction centers (sites) laying on planes which are used to build simple geometries. The chemical character of the pseudo atoms is specified by the 12–6 Lennard-Jones parameters ε_ss and σ_ss. The potential energy due to adsorbate-pore wall interaction was calculated by placing a probe species over one of the atoms in the array and summing over all interactions. Any probe at the same distance from the surface is given the same potential, regardless of its lateral position over the atoms. The parameters ε_ss and σ_ss were found by calibrating the model against a real material using heat of adsorption at zero adsorbate concentration.

In this work, the pore model is a cylinder of silicalitic nature whose potential parameters were determined using experimental data for Ar in the zeolite VPI 5. The chemical radius R' of the VPI 5 pore was taken to be $0.605\,\mathrm{nm}$ [26] giving a physical radius $R = 0.727\,\mathrm{nm}$ according to the relation:

$$R = R' + z_0 - \frac{\sigma_{\mathrm{Ar-Ar}}}{2}$$

where $z_0 = 0.8506\sigma_{\mathrm{Ar-O}}$ is the distance at which the Ar–O wall potential obtains its minimum value, and $\sigma_{\mathrm{Ar-Ar}} = 0.3405\,\mathrm{nm}$.

The isosteric heat of adsorption at zero coverage was calculated via the expression

$$q_\mathrm{st}(\rho \to 0) = k_\mathrm{B}T - \frac{\int_V \mathrm{d}\mathbf{r}\, u(\mathbf{r}) \exp(-\beta u(\mathbf{r}))}{\int_V \mathrm{d}\mathbf{r} \exp(-\beta u(\mathbf{r}))} \tag{10}$$

where $u(\mathbf{r})$ is the average potential energy of an isolated methane molecule over a large number of positions denoted by the vector $\mathbf{r}$ in the configurational space of pore volume V.

The measured experimental isosteric heat for Ar at 77K in VPI 5 is $q_\mathrm{st}(\rho \to 0) = 15.99\,k_\mathrm{B}T$ [22,26]. Evaluation of the integrals of Eq. (10) via Monte Carlo numerical integration, under the same conditions with the experiment, for a model cylinder consisting of one layer of oxide atoms [27] and using the reasonable value of $\sigma_\mathrm{ss} = 0.270\,\mathrm{nm}$, gave the calculated $q_\mathrm{st}(\rho \to 0) = 15.96\,k_\mathrm{B}T$ when $R = 0.729\,\mathrm{nm}$, and $\varepsilon_\mathrm{ss}/k_\mathrm{B} = 395\mathrm{K}$.

Grand Canonical Monte Carlo

Grand canonical Monte Carlo simulations were run at constant μ, V, T. The technique involves move, creation and destruction trials according to Metropolis scheme [28,29]; to ensure good statistics, the box size was altered so that an average number of not less than 500 molecules to be kept during the runs.

Adsorption isotherms are presented as plots of the fractional occupancy $\theta = \rho/\rho_\mathrm{s}$, (with the number density ρ_s being the maximum capacity of the pore of given radius to methane molecules), versus fugacity. Singled density distribution functions were collected by counting molecules into 100 concentric annulus of the same thickness inside the cylindrical pore model.

Equilibrium Molecular Dynamics

Transport properties were found from equilibrium molecular dynamics simulations carried out in both isolated (constant N, V, E) and isothermal systems (constant N, V, T) using a configuration obtained from a GCMC run as a starting point. In the case of (N, V, T), the system was thermostated by means of a Gaussian constrain kinetics [28,29].

From the EMD runs the self-diffusion coefficient D_s was calculated by employing Eqs. (6) and (7) after the master program having run for at least 2×10^4 time steps, and averages were collected over about 8×10^3 steps.

The corrected diffusion coefficient D_0 was calculated after the master EMD program having run for 4×10^5 time steps in order to allow statistically sufficient collection of averages (up to 1.5×10^5 time steps) via Eqs. (8) and (9). In cylindrical pores the components of the diffusion vector normal to the wall must be zero, so only the component in the flow direction (z-coordinate) was used in all calculations involved in the above Eqs..

In order to overcome the lack of a corrugated potential field a set of artificial boundary conditions were imposed. Therefore, the adsorbate molecule-wall collisions was modeled by using the diffuse boundary conditions method [21], namely randomizing the momentum of particles that have collided with the wall subject to the constrains: (i) the magnitude $|\mathbf{v}|^2$ of the velocity vector $\mathbf{v}$ remains unchanged and (ii) living the magnitude of the component of the velocity normal to the wall $|\mathbf{v}_r|^2$ constant. Vectors $\mathbf{v}_r$ and $\mathbf{v}_t$ (tangential at the point of collision), arise after the orthogonal transformation $(\mathbf{v}_x, \mathbf{v}_y, \mathbf{v}_z) \rightarrow (\mathbf{v}_r, \mathbf{v}_t, \mathbf{v}_z)$ over angle ϕ; then follows randomization according to the relations

$$|\mathbf{v}_t| = |\mathbf{v}_{tz}|\cos 2\pi\xi$$

$$|\mathbf{v}_z| = |\mathbf{v}_{tz}|\sin 2\pi\xi$$

where $|\mathbf{v}_{tz}|^2 = |\mathbf{v}|^2 - |\mathbf{v}_r|^2$ and ξ a normalized random number in the interval (0,1). Afterwards, vectors $\mathbf{v}_r$, $\mathbf{v}_t$ and $\mathbf{v}_z$ are retransformed to the original coordination system ($\mathbf{v}_x$, $\mathbf{v}_y$, $\mathbf{v}_z$) in order to proceed with the next dynamics step.

Further analytical studies about the nature of the flow and collisions near the wall in nanotubes can be found in [38–40].

Time steps t varied from 10^{-3} to 5×10^{-3} in reduced units, according to relation $t^* = t(\varepsilon/m\sigma^2)^{1/2}$, in all cases. Diffusivities were also expressed in reduced units according to $D^* = Dm^{1/2}\varepsilon^{-1/2}\sigma^{-1}$.

Dual Control Volume Grand Canonical Molecular Dynamics

The transport diffusion coefficient D_t, was found using a nonequilibrium molecular dynamics method. The simulation box was divided into three equal sections in the flow direction, and constant chemical potential were maintained in the two end sections by Metropolis Monte Carlo creation and destruction trials; molecular dynamics time steps were performed in all the molecules in the system in a way so that the ratio of stochastic trials to dynamics steps was fairly large (about 30 to 60), resulting in a concentration gradient between the two end sections of constant density at steady state.

Two methods were followed in order to handling molecules that passed through the end sections of the box in the flow direction during a dynamic step: (a) The molecules outside the box were removed from the simulation; (b) the component of the velocity vector in the direction of flow was reversed at the next time step for those molecules that had passed through these boundaries. Since for the cylindrical simulation box of this work condition (a) enabled lower level of noise in the region close to boundaries at both local volumes, it was preferred in the runs presented in this paper.

By counting the total number of particles lost N_- and gained N_+ in each end section and after applying mass balance condition, the molecular flux was obtained by the form:

$$\mathbf{J} = \frac{1}{A_c}\frac{\mathrm{d}(N_+ - N_-)}{\mathrm{d}t} \tag{11}$$

where A_c is the cross sectional area of the pore. Flux was calculated through Eq. (11) by plotting $N_+ - N_-$ against time.

The flux at any cross section is related to the $\mathbf{r}_a$ component of the velocity of the local center of mass $\mathbf{u}_a(\mathbf{r}_a)$ (local streaming velocity) by

$$\mathbf{J} = \rho(\mathbf{r}_a)\mathbf{u}_a(\mathbf{r}_a) \tag{12}$$

Since flux is constant in steady state flow, $\mathbf{u}_a(\mathbf{r}_a)$ can be found from Eq. (12). Each molecule at $\mathbf{r}_a$ possesses this extra streaming velocity component. After a suitable settling time, the calculated streaming velocities in the end sections were added to newly created particles to ensure that creations are compatible with molecular transport. Subsequently, the streaming velocity was updated every 3–5 dynamic steps. Similarly the local streaming velocity was subtracted from the apparent total velocity of each molecule before applying a Gaussian constraint to correct temperature.

An effective (transport) diffusion coefficient D_t at steady state was then calculated from the equation

$$\int_{x=0}^{x=\ell} J\,\mathrm{d}x = J\ell = \int_{x=0}^{x=\ell} D d\rho = D_{\mathrm{t}}(\rho_{x=\ell} - \rho_{x=0}) \qquad (13)$$

where ℓ is the length over which the density gradient is created. Thus, from Eq. (13) is seen that transport diffusivity represents an integral coefficient D_{t} rather than a differential coefficient as the pure Fickian coefficient D.

Most of the runs of this work carried out on a Beowulf linux cluster (12 Athlon-MP CPUs). The run time performance on this machine for a number of molecules up to 500 was about 1.7 days for 5×10^8 time steps.

RESULTS AND DISCUSSION

Molecular Dynamics

In Fig. 1, the simulated isotherms obtained via GCMC are shown for the three sizes of the sorbent model. The above sizes have been chosen, in order three cases of density distribution to be studied as can be seen in Fig. 3; namely, in the pore with the radius of 0.585 nm, molecules are highly localized close to the wall; for the radius of 0.681 nm filling of central section commences, and for the radius of 0.780 nm formation of a second molecular layer localized in the pore center is henceforth favored.

In Fig. 2, the MD results for the model pores employed are presented. It is seen that the self-diffusivity D_{s} decreases with the increase of adsorbate loading as expected due to increase of the intermolecular collisions. The transport diffusion coefficient D_{t}, rises steeply a little before the completion of the monolayer as can be seen from Fig. 1, following the same trend with the transport diffusivity calculated from D_0. This finding, being in agreement with earlier observation in graphitic

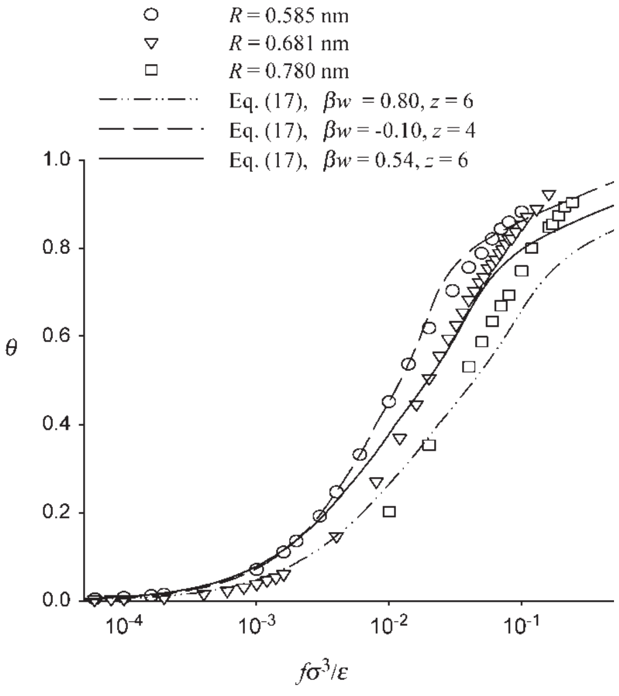

FIGURE 1 GCMC isotherms of CH_4 at 298 K in cylindrical silica pores of various sizes (points); isotherms according to Quasichemical theory (lines).

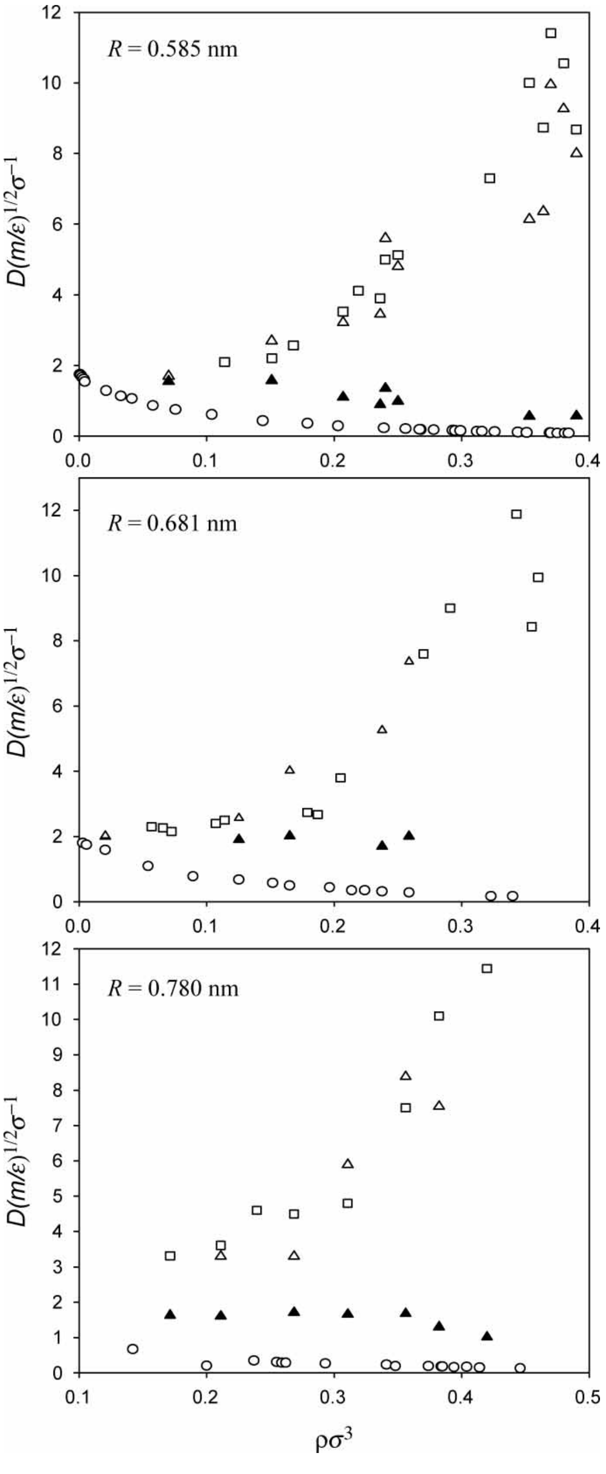

FIGURE 2 Results of self- (circles), corrected (filled triangles), DCV GCMD transport (squares) and EMD transport (open triangles) diffusivities of CH_4 in cylindrical silica pores.

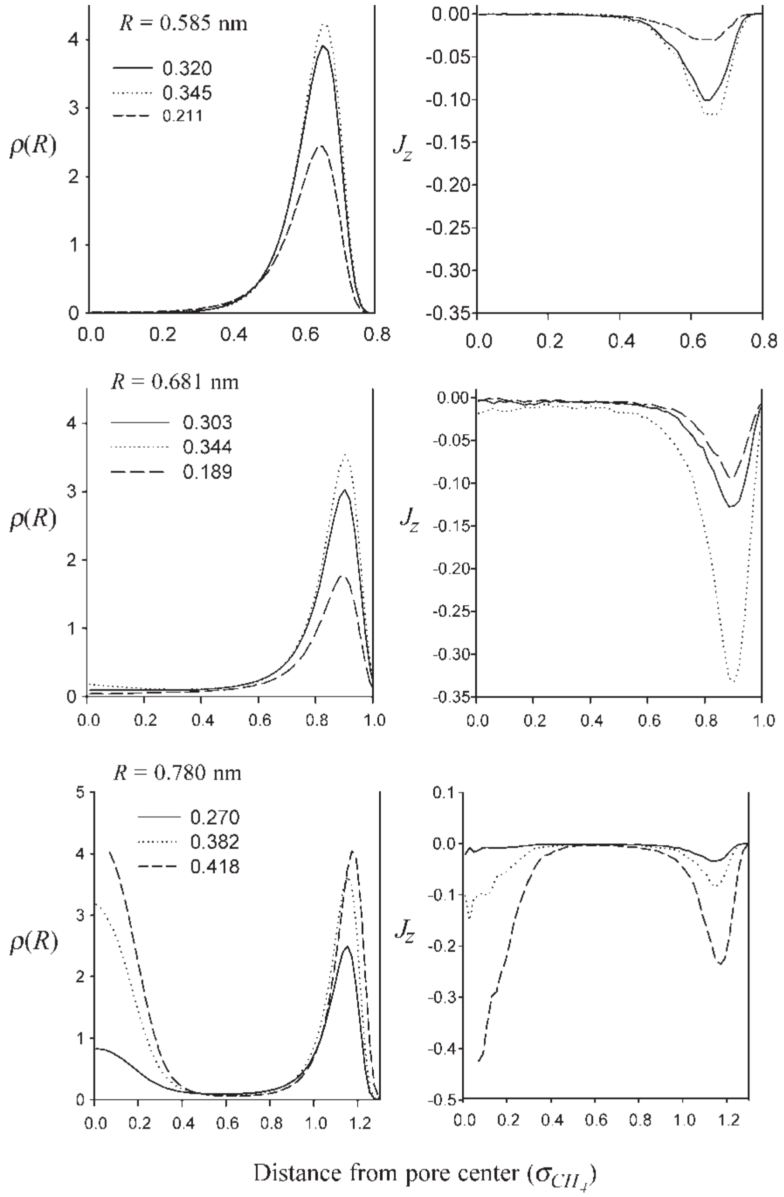

FIGURE 3 Results of single density distribution function (left column) and flux distribution from DCV GCMD (right column), along the pore radius for the models used, at various adsorbate number densities.

slit pores [11,24,25,30,31], may be attributed to flow cooperative effects. The flux distribution along the pore diameter shown in Fig. 3, especially in the larger sizes, supports this evidence. It must be noted that in all cases flux values appear negative as a result of the original convention made up in the programming code where the direction of flow was always toward the negative direction of z-axis. An extensive discussion about the hydrodynamic origin and viscous effects of transport in nanoporous structures are found in [33,37].

No significant discrepancy between the transport diffusivities calculated from Darken relation through the corrected diffusivity D_0, from equilibrium MD and the ones calculated directly from DCV GCMD, is observed. The noise in all graphs of Fig. 2, may be due to poor statistics involved in the calculation of the collective property D_0 along with the computational difficulties in executing molecular dynamics in so highly constricted pores [21]. The agreement of the two methods EMD and DCV GCMD in predicting transport diffusivity has also been verified in the works of Maginn and co-workers [32] and Bhatia and Nicholson [33].

The transport diffusivity D_t, in the pores of 0.585 and 0.681 nm appears a slight maximum at high densities well after the monolayer completion indicating higher viscous contribution. In the smaller size, it is not clear whether this is meaningful or just a result of the intrinsic statistical noise at high densities of the DCV GCMD method. In the wider pore of 0.780 nm, such a trend is not observed at number densities up to 0.45. In that size, as density increases application of DCV GCMD becomes problematic due to enhanced difficulties in achieving a devoid of noise density profile across the pore ends.

Quasichemical Approach to Adsorption

The simulation results were compared against the predictions of the quasichemical theory (QC), which is a mean field approximation due to Guggenheim for the study of the thermodynamics of non-ideal solutions [34]. In this work, we have adapted the QC theory in order to analyze a "solution" of N_{A} adsorbate molecules distributed among a total of N_{s} adsorption sites arranged on a simple lattice of coordination number z. Each lattice site is capable of accommodating at most one molecule. Each sorbate molecule interacts with its nearest neighbours. The total number of nearest neighbour pairs is denoted by N_{AA}; the contribution from each pair of nearest neighbour sorbed molecules to the overall potential energy is w_{AA}. In the following, we will use the quantity $w = zw_{\mathrm{AA}}/2$ for convenience. With these definitions, the potential energy U_{AA} of sorbate–sorbate interactions reads

$$U_{\mathrm{AA}} = N_{\mathrm{AA}}\frac{2w}{z} \tag{14a}$$

For a given number of sorbate molecules, N_{A}, on the N_{s} sites, there are

$$\binom{N_{\mathrm{s}}}{N_{\mathrm{A}}} = \frac{N_{\mathrm{s}}!}{N_{\mathrm{A}}!(N_{\mathrm{s}} - N_{\mathrm{A}})!}$$

arrangements on the lattice. The value of N_{AA}, and hence the energy U_{AA}, may vary among these configurations. We now introduce a mean field approximation, where all configurations of N_{A} molecules are assigned the same energy,

$$\langle U_{\mathrm{AA}}\rangle = \frac{2w\langle N_{\mathrm{AA}}\rangle}{z} \tag{14b}$$

Furthermore, we consider the system in the grand canonical ensemble at temperature T, at equilibrium with a bulk fluid phase where the chemical potential of the sorbate is μ. The grand partition function $\Xi(\mu,V,T)$ of the adsorbed molecules in the lattice can be written as follows

$$\Xi(\mu, V, T) = \sum_{N_{\mathrm{A}}=0}^{N_{\mathrm{s}}} \exp(-\beta\langle U_{\mathrm{AA}}\rangle) \times \binom{N_{\mathrm{s}}}{N_{\mathrm{A}}} \exp(N_{\mathrm{A}}\beta\mu)[q^{\mathrm{s}}(T)]^{N_{\mathrm{A}}} \tag{15}$$

where $q^{\mathrm{s}}(T)$ is the partition function over the internal degrees of freedom of an adsorbed molecule on the lattice, referred to the lowest-energy internal state of the molecule in the gas phase at infinite separation. The mathematical method for estimating the mean pair energy $\langle U_{\mathrm{AA}}\rangle$ from Eq. (15) is due to Bethe [35], resulting eventually in the relation

$$\langle U_{\mathrm{AA}}\rangle = wN_{\mathrm{A}}\left(1 - \frac{2-2\theta}{\zeta+1}\right)$$

where ζ is defined by the expression

$$\zeta = \{1 - 4\theta(1-\theta)[1 - \exp(-2\beta w/z)]\}^{1/2} \tag{16}$$

Through the grand partition function, using elementary statistical mechanics, and equating the chemical potentials of the bulk and sorbed phase, the isotherm of the system can be derived, resulting in the following relations

$$\frac{\beta\Lambda^3 q^{\mathrm{s}}(T)}{q} f = bf = \frac{\theta}{1-\theta}\left(\frac{2-2\theta}{\zeta+1-2\theta}\right)^z \tag{17}$$

where q is the partition function over the internal degrees of freedom in the ideal gas, Λ is the thermal wavelength and the parameter b is related to the Henry's constant K_{H} for sorption through the expression

$$b = \lim_{f\to 0}\frac{\theta}{f} = \frac{1}{\rho_{\mathrm{m}}}\lim_{f\to 0}\frac{\rho}{f} = \frac{1}{\rho_{\mathrm{m}}}K_{\mathrm{H}}$$

Consequently, the thermodynamic factor in Eq. (5) becomes

$$\frac{\mathrm{d}\ln f}{\mathrm{d}\ln\theta} = 1 + \frac{\theta(1-z)}{1-\theta} - \frac{2\theta z}{\zeta+1-2\theta}\left[\frac{1-\exp(-2\beta w/z)}{\zeta} - 1\right]$$

Obviously, for no sorbate–sorbate interactions ($w = 0$) the QC isotherm degenerates into the simpler Langmuir isotherm:

$$bf = \frac{\theta}{1-\theta} \tag{18}$$

In Fig. 1, three theoretical QC isotherm curves are shown for the reasonable b values of 0.003, 0.011 and 0.019, estimated at infinite adsorbate dilution for the pore radii of 0.585, 0.681 and 0.780 nm, respectively, corresponding to the dimensionless values of -0.10, 0.54 and 0.80 for the energy w. These curves, act as an ideal reference for each of the aforementioned capillaries, indicating a more attractive intermolecular energy ($w < 0$) for the narrower spaces which becomes much weaker ($w > 0$) as pore size increases. Thus, the energy w as deduced from the derivation of Eqs. (14b) and (15), expresses indirectly the nature of the potential field of the confined phase inside a nanopore, namely it reflects the energetic topology of the pore lattice.

A sorbent lattice characterized by a uniform coordination number z, is obviously far from the real situation as can be seen clearly in Fig. 3 from the calculated methane density distribution functions inside the pores; the deviation of simulation points from the theoretical curves in high occupancies, in Fig. 1 supports this argument too. However, the QC approximation even under the oversimplification regarding the sorbent lattice, can be utilized in order to introduce an additional parameter for the pair interactions in the simple thermodynamics of Langmuir type (see Eq. (18)), obtaining Eq. (17), which in turn can be furthermore exploited in order to give an interpretation of the loading dependence of diffusivity (see next section).

Occupancy Dependence of Corrected Diffusivity

A first attempt to relate sorbate–sorbate energetics in the adsorbed phase to the occupancy dependence of D_0 has been made by Reed and Ehrlich [36]. Their model has originally been developed for surface diffusion on a regular lattice of sites, where the overall effective jump rate $\mathcal{G}(\theta)$ of the adsorbed molecules on a simple lattice is written as a function of $\mathcal{G}^{(i)}$, the individual jump rate of a molecule surrounded by i adsorbate molecules at nearest neighbour sites, and of the probability $P^{(i)}$ that such a molecule is surrounded by i neighbours. The latter quantity is estimated by invoking the QC approximation, giving

$$P^{(i)} = \binom{z}{i}\left[\zeta - 1 + 2\theta\right]^{i}[2 - 2\theta]^{z-i}\left[\zeta + 1\right]^{-z} \tag{19}$$

In expressing $\mathcal{G}^{(i)}$, it is assumed that any attempt to jump into an already occupied site is unsuccessful. The overall effective jump rate emerges as

$$\mathcal{G}(\theta) = \mathcal{G}(0) \times \left[\frac{\zeta+1}{2-2\theta}\right]^{-z}\left[1 + \frac{\zeta - 1 + 2\theta}{2-2\theta}\exp(2\beta w/z)\right]^{z-1} \tag{20}$$

where $\mathcal{G}(0)$, the jump rate on an empty lattice, is the limiting value of Eq. (20) as θ approaches zero.

Calculating the flux vector of the adsorbed molecules executing jumps of constant length λ on the lattice, with the chemical potential gradient acting as a driving force, and comparing with Eq. (4), the following relation for the transport diffusivity is derived

$$D_t(\theta) = \mathcal{G}(\theta)\lambda^2\frac{\partial \ln f}{\partial \ln \theta} \tag{21}$$

In the limit of very low loadings, by combining Eqs. (5), (20) and (21), one obtains the relations

$$D_t(0) = D_0(0) = \mathcal{G}(0)\lambda^2 \tag{22}$$

Combination of Eqs. (5), (20)–(22) leads to the following expression for the occupancy dependence of the corrected diffusivity on a lattice of coordination number z,

$$D_0(\theta) = D_0(0) \times \left[\frac{\zeta+1}{2-2\theta}\right]^{-z}\left[1 + \frac{\zeta - 1 + 2\theta}{2-2\theta}\exp(2\beta w/z)\right]^{z-1} \tag{23}$$

For $w = 0$ (no sorbate–sorbate interaction apart from the requirement of no multiple occupancy of sites), Eq. (23) takes the simple form

$$D_0(\theta) = D_0(0)(1 - \theta) \tag{24}$$

Our simulation estimates for the diffusivities $D_0(\theta)$ for CH_4 in the three models, normalized by the corresponding $D_0(0)$ values extracted from Fig. 2, are presented in Fig. 4. The theoretical $D_0(\theta)/D_0(0)$ curves obtained from Eq. (23), after inserting the values of w found in the previous section, are shown to be very close to the corresponding simulation points depicted in the same figure, providing a plausible explanation of the D_0 behaviour on the basis of the strength of sorbate–sorbate interactions.

An analogous finding of Krishna and co-workers regarding CH_4/CF_4 mixtures diffusivity in MFI zeolite, based on molecular dynamics and the Maxwell–Stefan formulation can be found in [41]. Also, a recent experimental and simulation study of

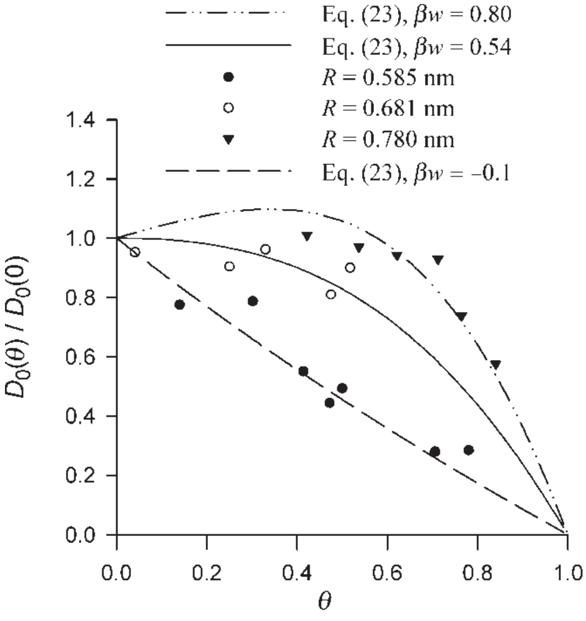

FIGURE 4 Normalized corrected diffusivities from EMD (points) and QC theoretical curves obtained from the R–E model (see text) for the pair interaction energy values extracted from the procedure of figure 1, as a function of fractional occupancy.

the CF_4 diffusivity loading dependence in silicalite of Jobic *et al.* is reported in [42].

CONCLUSIONS

The dependence of self-, transport and corrected diffusivity of methane in three cylindrical silica models, calibrated with respect to zeolite VPI 5, upon the sorbate concentration was studied using standard equilibrium molecular dynamics and dual control volume grand canonical molecular dynamics. The two methods showed no significant difference in predicting transport diffusivities.

Mapping the predicted grand canonical Monte Carlo thermodynamics onto the quasichemical model, which assumes adsorption on a lattice of discrete sites and invokes a mean field approximation to estimate the number of nearest-neighbour pairs, led to the conclusion that sorbate–sorbate interactions are considerably stronger (more attractive, w tends to negative values) as the pore width decreases.

While the self-diffusivity variation with sorbate loading and pore size is directly explainable in terms of the frequency of intermolecular collisions which increases as concentration (pore width) increases (decreases), causing degrease to D_s, the transport diffusivity trend needs a more extensive elaboration since it comprises a thermodynamic and a kinetic part (see Eq. (5)). Thus, a more precise thermodynamic factor $\mathrm{d}\ln f\ /\mathrm{d}\ln\theta$ introduced in this work, which includes sorbate–sorbate interactions, was inserted to Eq. (5) reflecting the quasichemical sorption thermodynamics contribution to D_t.

To understand the physical origin of the loading dependence of the kinetic part of Eq. (5), D_0, the model of Reed and Ehrlich [36] was adapted with the parameters obtained from the procedure shown in Fig. 1. The conclusion is that, in the narrower pores the sorbent lattice causes attractive pair interaction energy to sorbate molecules (w strength negative in the model), leading to clearly decreasing $D_0(\theta)$, whereas in the wider pores where the attraction is weaker (w strength positive in the model) an almost constant $D_0(\theta)$ is obtained (see Fig. 4).

Although the model is but a crude representation of actual transport in nanopores, with the mapping procedure adapted in this work it captures the different simulated diffusivity dependencies satisfactorily, providing a simple qualitative explanation of the corrected diffusivity trend, and pointing out that differences in sorbate–sorbate energetics emerge as the physical reason for the different occupancy and pore width dependence of the corrected and transport diffusivity. Indeed, the development of a model involving multiple coordination numbers as well as interaction energy parameters depending on the local environment of a nanoporous medium, which was out of the scope of the present paper, is a strong incentive for further work in this field.

Acknowledgements

I wish to express my gratitude to Prof. David Nicholson for his invaluable support on the DCV GCMD technique during my stay at Imperial College. This work was partially supported by the European project TROCAT (Contract No. G5RD-CT-2001-00520).

References

[1] Magda, J.J., Tirrell, M. and Davis, H.T. (1985) "Molecular dynamics of narrow, liquid-filled pores", *J. Chem. Phys.* **83**, 1888.

[2] MacElroy, J.M.D. and Suh, S.-H. (1987) "Computer simulation of moderately dense hard sphere fluids and mixtures in microcapillaries", *Mol. Phys.* **60**, 475.

[3] Cracnell, R.F. and Gubbins, K.E. (1993) "Molecular simulation of adsorption and diffusion in VPI 5 and other aluminophosphates", *Langmuir* **9**, 824.

[4] Maginn, E.J., Bell, A.T. and Theodorou, D.N. (1993) "Transport diffusivity of methane in silicalite from equilibrium and nonequilibrium simulations", *J. Phys. Chem.* **97**, 4173.

[5] Theodorou, D.N., Snurr, R.Q. and Bell, A.T. (1999) "Comprehensive supramolecular chemistry", In: Alberti, G. and Bein, T., eds, *Molecular Dynamics and Diffusion in Microporous Materials* (Pergamon), Vol. 7.

[6] Makrodimitris, K., Papadopoulos, G.K. and Theodorou, D.N. (2001) "Prediction of permeation properties of CO_2 and N_2 through silicalite via molecular simulations", *J. Phys. Chem. B* **105**, 777, and references therein.

[7] Pellenq, R.J-M. and Nicholson, D. (1994) "Intermolecular potential function for the physical adsorption of rare gases in silicalite", *J. Phys. Chem.* **98**, 13339.

[8] Steele, W.A. (1973) "Physical interaction of gases with crystalline solids.1. Gas–solid energies and properties of isolated adsorbed atoms", *Surface Sci.* **36**, 317.

[9] Steele, W.A. (1974) *The Interaction of Gases with Solid Surfaces* (Pergamon Press, Oxford).

[10] Nicholson, D. and Gubbins, K.E. (1995) "Separation of carbon dioxide–methane mixtures by adsorption: effects of geometry and energetics on selectivity", *J. Chem. Phys.* **104**, 8126.

[11] Cracknell, R.F., Nicholson, D. and Quirke, N. (1995) "Direct molecular dynamics simulation of flow down a chemical potential gradient in a slit shaped micropore", *Phys. Rev. Lett.* **74**, 2463.

[12] Nicholson, D. (1998) "Simulation studies of methane transport in model graphite micropores", *Carbon* **36**, 1511.

[13] Papadopoulos, G.K., Jobic, H. and Theodorou, D.N.T. (2004) "Transport diffusivity of N_2 and CO_2 in silicalite: coherent quasielastic neutron scattering measurements and molecular dynamics simulations", *J. Phys. Chem. B* **108**, 12748.

[14] Evans, D.J. and Morris, G.P. (1990) *Statistical Mechanics of Nonequilibrium Liquids* (Academic Press, San Diego).

[15] Papadopoulou, A., Becker, E.D., Lupkowski, M. and Van Swol, F. (1993) "Molecular dynamics and Monte Carlo simulations in the grand canonical ensemble: local versus global control", *J. Chem. Phys.* **98**, 4897.

[16] Heffelfinger, G.S. and van Swol, F. (1994) "Diffusion in Lennard–Jones fluids using dual control volume grand canonical molecular dynamics simulation (DCV-GCMD)", *J. Chem. Phys.* **100**, 7548.

[17] MacElroy, J.M.D. (1994) "Nonequilibrium molecular dynamics simulation of diffusion and flow in thin microporous membranes", *J. Chem. Phys.* **101**, 5274.

[18] Pohl, P.I., Heffelfinger, G.S. and Smith, D.M. (1996) "Molecular dynamics computer simulation of gas permeation in thin silicalite membranes", *Mol. Phys.* **89**, 1725.

[19] MacElroy, J.M.D. and Boyle, M.J. (1999) "Nonequilibrium molecular dynamics simulation of a model carbon membrane separation of CH4/H-2 mixtures", *Chem. Eng. J.* **74**, 85.

[20] Travis, K.P. and Gubbins, K.E. (1999) "Transport diffusion of oxygen–nitrogen mixtures in graphite pores: a nonequilibrium molecular dynamics (NEMD) study", *Langmuir* **15**, 6050.

[21] Papadopoulos, G.K., Suh, S.-H. and Nicholson, D. (1999) "Molecular dynamics studies of diffusion in model cylindrical pores at very low densities", *Mol. Simul.* **22**, 237.

[22] Hathaway, P.E. and Davis, M.E. (1990) "High resolution quasi-equilibrium sorption studies of molecular sieves", *Catal. Lett.* **5**, 1333.

[23] Suh, S.-H. and Nicholson, D. (2001) "A simulation study of the effects of adsorbent energy on the diffusion of molecules in slit pores: 1 commensurate slit widths", *Mol. Phys.* **99**, 383.

[24] Nicholson, D. (1997) "The transport of adsorbate mixtures in porous materials: basic equations for pores with simple geometry", *J. Mem. Sci.* **129**, 209.

[25] Cracknell, R.F., Nicholson, D. and Gubbins, K.E. (1995) "Molecular dynamics study of the self-diffusion of supercritical methane in slit shaped graphitic micropores", *J. Chem. Soc. Faraday Trans.* **91**, 1377.

[26] Davis, M.E. (1989) "Physicochemical properties of VPI 5", *J. Am. Chem. Soc.* **111**, 3919.

[27] Kiselev, A.V., Lopatcin, A.A. and Shulga, A.A. (1985) "Molecular statistical calculation of gas adsorption by silicalite", *Zeolites* **5**, 261.

[28] Nicholson, D. and Parsonage, N.G. (1982) *Computer Simulation and the Statistical Mechanics of Adsorption* (Academic Press, London).

[29] Allen, M.P. and Tildesley, D.J. (1987) *Computer Simulation of Liquids* (Clarendon Press, Oxford).

[30] Nicholson, D., Cracnell, R.F. and Quirke, N. (1996) "A transition in the diffusivity of adsorbed fluids through micropores", *Langmuir* **12**, 4050.

[31] Nicholson, D. and Travis, K. (2000) In: Kanellopoulos, N.K., eds, *Recent Advances in Gas Separation by Microporous Ceramic Membranes, Membrane Science and Technology Series* (Elsevier, Amsterdam) **6**, p 257.

[32] Arya, G., Maginn, E.J. and Chang, H.-C. (2001) "A critical comparison of equilibrium, non-equilibrium and boundary-driven molecular dynamics techniques for studying transport in microporous materials", *J. Chem. Phys.* **115**, 8112.

[33] Bhatia, S.K. and Nicholson, D. (2003) "Molecular transport in nanopores", *J. Chem. Phys.* **119**, 1719.

[34] Fowler, R. and Guggenheim, E.A. (1949) *Statistical Thermodynamics* (University Press, Cambridge).

[35] Bethe, A. (1935), *Proc. Roy. Soc. A* **150**, 552.

[36] Reed, D.A. and Ehrlich, G. (1981) "Surface diffusion, atomic jump rates and thermodynamics", *Surf. Sci.* **102**, 588.

[37] Bhatia, S.K. and Nicholson, D. (2003) "Hydrodynamic origin of diffusion in nanopores", *Phys. Rev. Lett.* **90**, 016105.

[38] Sokhan, V.P., Nicholson, D. and Quirke, N. (2002) "Fluid flow in nanopores: accurate boundary conditions for carbon nanotubes", *J. Chem. Phys.* **117**, 8531.

[39] Sokhan, V.P., Nicholson, D. and Quirke, N. (2001) "Fluid flow in nanopores: an examination of hydrodynamic boundary conditions", *J. Chem. Phys.* **115**, 3878.

[40] Arya, G., Chang, H.-C. and Maginn, E.J. (2003) "Molecular simulations of Knudsen wall-slip: effect of wall morphology", *Mol. Simul.* **29**, 697.

[41] Skoulidas, A.I., Sholl, D.S. and Krishna, R. (2003) "Correlation effects in diffusion of CH4/CF4 mixtures in MFI zeolite. A study linking MD simulations with the Maxwell–Stefan formulation", *Langmuir* **19**, 7977.

[42] Jobic, H., Skoulidas, A.I. and Sholl, D.S. (2004) "Determination of concentration dependent transport diffusivity of CF_4 in silicalite by neutron scattering experiments and molecular dynamics", *J. Phys. Chem. B* **108**, 10613.